Available online at www.sciencedirect.com
ScienceDirect
Trans. Nonferrous Met. Soc. China 19(2009) 1−8
Transactions of Nonferrous Metals Society of China
www.tnmsc.cn

Effect of sample diameter on primary dendrite spacing of directionally solidified Al-4%Cu alloy

QU Min(屈 敏), LIU Lin(刘 林), TANG Feng-tao(唐峰涛), ZHANG Jun(张 军), FU Heng-zhi(傅恒志)

State Key Laboratory of Solidification Processing, Northwestern Polytechnical University, Xi'an 710072, China

Received 19 May 2008; accepted 22 September 2008

Abstract: The relationship between primary dendrite arm spacing and sample diameter was studied during directional solidification for Al-4%Cu (mass fraction) alloy. It is shown that primary dendrite spacing is decreased with the decrease of the sample diameter at given growth rate. By regressing the relationship between primary dendrite arm spacing and the growth rate, the primary dendrite arm spacing complies with $461.76v^{-0.53}$, $417.92v^{-0.28}$ and $415.83v^{-0.25}$ for the sample diameter of 1.8, 3.5 and 7.2 mm, respectively. The primary dendrite spacing, growth rate and thermal gradient for different sample diameters comply with $28.77v^{-0.35}G^{-0.70}$, $23.17v^{-0.35}G^{-0.70}$ and $23.84v^{-0.35}G^{-0.70}$, respectively. They are all consistent with the theoretical model $\lambda_1 = k_b v^{-a_1} G^{-b_1}$, and b_1/a_1=2. By analyzing the experimental results with classical models, it is shown that KURZ-FISHER model fits for the primary dendrite spacing in smaller sample diameters with weaker thermosolute convection. Whereas TRIVEDI model is suitable for describing primary dendrite arm spacing with a larger diameter (d＞2 mm) where convection should be considered.
Key words: directional solidification; sample diameter; primary dendrite arm spacing; thermal gradient

1 Introduction

Primary dendrite spacing is one of the parameters which can describe the scales of the solidification microstructure in solidification field. At present, extensive studies on primary dendrite spacing have been performed not only for metallic materials[1−4], but also for transparent organic substance[5−7]. Moreover, the monotropic function[8−11] of the primary dendrite and solidification parameters of thermal gradient G, growth rate v and concentration c_0 has been gained right from the samples with an invariable size. Subsequently, analysis of a linear stability was made by WARREN and LANGER[12−13] for dendrite arrays, to obtain an analytic solution of primary dendrite spacing. However, these equations have been rarely used in the calculation of real alloy systems due to their complexity. HUNT and LU[14] investigated the cell/dendrite spacing by defining proper relevant dimensionless parameters, and they established a reliable numerical solution to the cell/dendrite spacing, which is suitable to primary spacing both for lower and higher velocity. Unfortunately, the sample diameter was not considered in their calculation.

The study for a variant diameter of specimens has been regarded during directional solidification in recent years. CHEN et al[15] have studied Pb-2.2%Sb and Al-2%Cu (mass fraction) alloy with different sample diameters, and it is recognized that macro-segregation is observed in the solidified direction resulted from the presence of convection. The research on the effect of convection with different diameters was performed [16−18], and the critical value of sample diameter(d＜2 mm) has been obtained when the convection can be ignored. The above works are both concerned on convection. But presently, there are few papers about primary dendrite spacing of different sample diameters yet, and the study of the effect of sample diameter on primary dendrite spacing has not built either. The sample diameter would affect the primary dendrite arm spacing, and the model about primary dendrite arm spacing considering the effect of sample diameter cannot only play a significant instructional role in theoretic calculation, but also play a role of forecast to experiment.

Therefore, in the present work, the variation of primary dendrite spacing of Al-4%Cu (mass fraction) alloy caused by different sample diameters was studied,

Foundation item: Project(50771081) supported by the National Natural Science Foundation of China
Corresponding author: QU Min; Tel: +86-29-88492227; E-mail: qm_021@yahoo.com.cn
DOI: 10.1016/S1003-6326(08)60220-4

and the experimental results were compared with theoretic models in order to achieve the effect of sample diameter on the primary dendrite spacing, and the classical models are divided for different sample diameters.

2 Experimental

Al-4%Cu (mass fraction) alloy was prepared by pure Al (99.99%) and Al-51.87%Cu (mass fraction) alloy in a vacuum induction melting furnace. The homogeneous liquid was cast into a wax mould with a cavity of 3.5 mm and 7.2 mm in diameter, and 150 mm in length. The surface was polished glossily and cleaned using an acetone before the experiment. Directionally solidified experiments were carried out in Bridgman apparatus which was heated by electric resistant furnace, as shown in Fig.1. Two Pt/Pt-13%Rh thermocouples with different lengths were used to record the temperature at upper and lower part of the furnace. The heating temperature was set at 1 000 ℃. The sample temperature was measured by a 0.25 mm K-typed NiCr/NiSi thermocouple which was placed inside an alumina tube (0.8 mm in inner diameter, 1.2 mm in outer diameter) and coated by alumina on its tip. Before heating, the thermocouple was put in parallel with the heat flow direction inside the crucible. As the specimen was melted, the thermocouple was fallen and kept onto the liquid/solid interface stayed at 1 000 ℃ for 30 min. Then, sample was withdrawn and the temperature was recorded by LR100 recorder simultaneously. Moreover, the thermocouple descended in accordance with specimen during the whole process. The temperature gradient was calculated from cooling curve measured by the recorder.

Specimens were withdrawn over a wide range of constant velocities. With a predetermined distance, they were quenched into water by pneumatic plant. Generally, the withdrawal rate was regarded to be equal to growth rate under steady state in most circumstances.

The solidified samples were longitudinally and transversally treated to study the solidification microstructure. They were then polished and etched by H_2O+HNO_3+HF corrosive solution. A Lecia DM4000 optical microscope was used to observe metallurgical structures, and the metallographic analytical microsoft SISC IAS V8.0 was applied to measure primary dendrite spacing. Usually, some dendrite arrays are angled to dendrite growth direction 〈100〉, therefore, the cross sections cannot exactly represent primary dendrite arm spacing. In this work, a calculating method was introduced, as shown in Fig.2. Namely, first the deviation of the dendrite array to its axis in their longitudinal sections was measured, then a calculation with the so-called primary dendrite spacing λ' was made. From the geometrical calculation, the equation $\lambda=\lambda'\sin\theta$ is obtained finally. The values of λ' were measured on the cross section by area counting method, at least on five different regions for each specimen. λ' is equal to $(1/M)(A/N)^{0.5}$, where M is the magnification factor, A is the total specimen cross section area and N is the number of primary dendrites on the cross section. For each region, N was larger than 50 to make sure the precise value of λ'. Finally, the mathematical statistics were applied to get the valuable λ'.

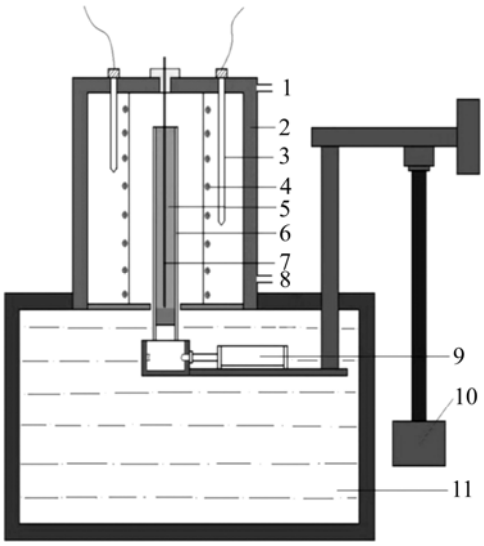

Fig.1 Sketch of Bridgman resistance heating directional solidification apparatus: 1—Water outlet; 2—Water cooling jacket; 3—B-type thermocouple; 4—Resistance wire; 5—Sample; 6—Alumina tube; 7—K-type thermocouple; 8—Water input; 9—Pneumatics; 10—Withdrawal device; 11—Water tank

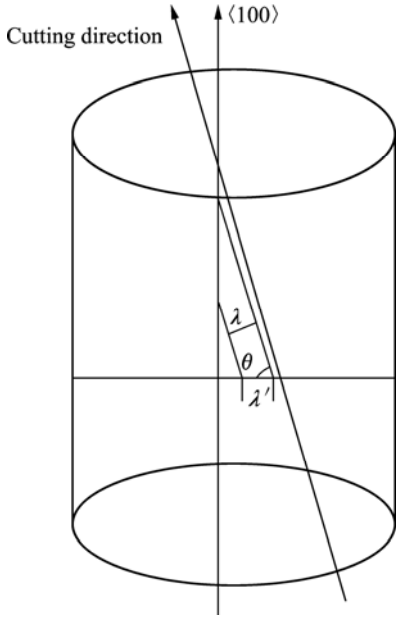

Fig.2 Measurement of primary dendrite spacing λ

3 Experimental results

3.1 Effect of sample diameter on evolution of liquid/solid interface

Fig.3 shows the quenched liquid/solid interface under different growth rates. As the growth rate is increased from 15 μm/s to 600 μm/s, the interface morphology varies from cellular to cellular-dendrite, then to coarse dendrite, and finally evolves to fine dendrite.

At the same growth rate, as for different diameters of the sample, the quenched interface is different, as shown in Fig.4. The smaller the sample diameter, the more stable the cellular interface is. For both 1.8 mm and 3.5 mm samples, their quenched interfaces are mainly cellular. But, in the 7.2 mm sample, some dendrites are found. For dendrite interface, its branch with a small diameter is not so strong as that with a larger one. This indicates that the stability of liquid/solid interfaces is improved for smaller diameter of samples.

3.2 Effect of sample diameter on primary dendrite arm spacing

With the measurement of primary spacing for different diameters under various growth rates, the values of PDAS (primary dendrite arm spacing) are derived, as listed in Table 1. It is deduced that the higher the growth rate, the smaller the PDAS is. By plotting PDAS versus growth rate, the value of primary spacing is found to

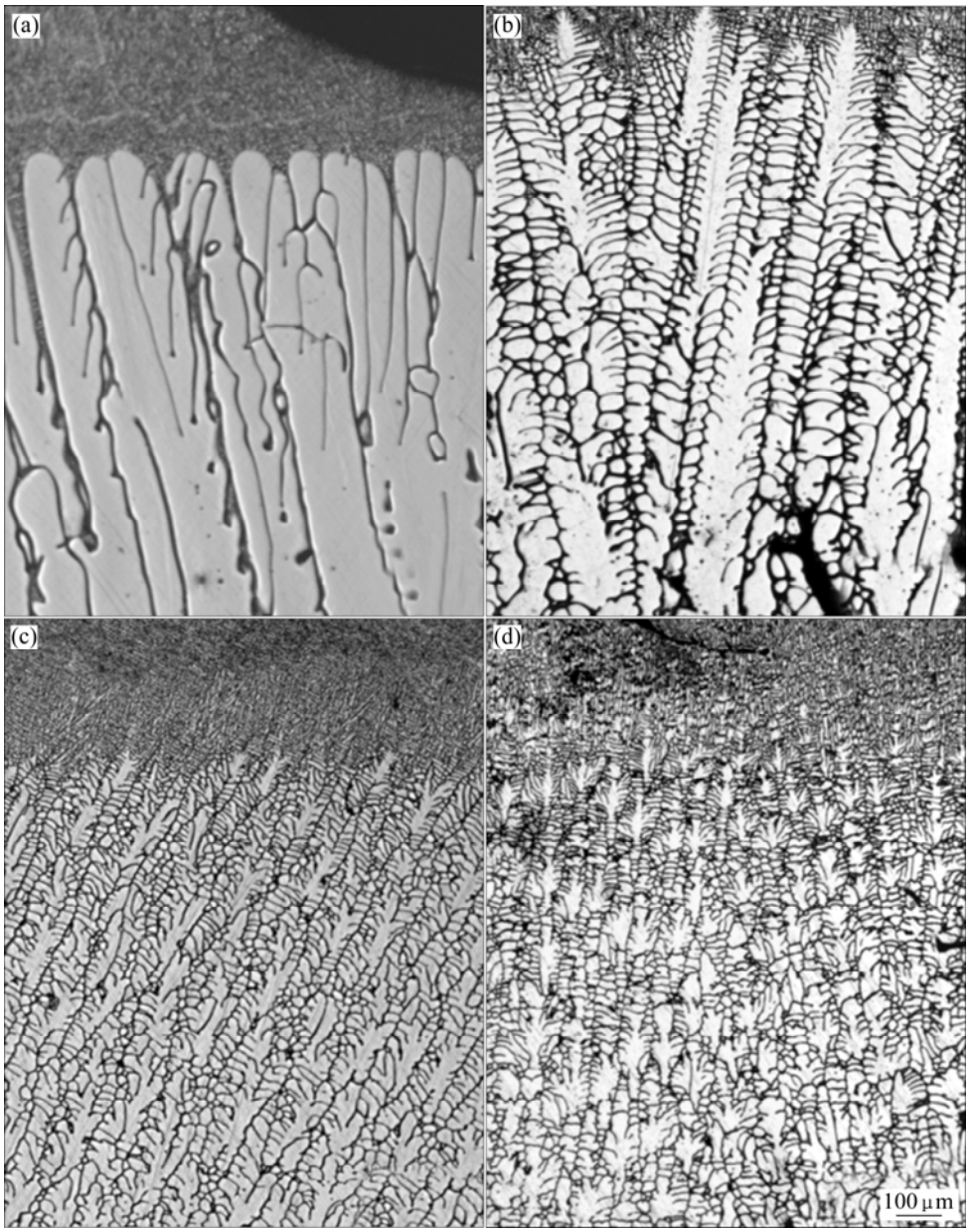

Fig.3 Morphologies of longitudinal sections of samples with various growth rates (d=3.5 mm): (a) v=15 μm/s; (b) v=100 μm/s; (c) v=300 μm/s; (d) v=600 μm/s

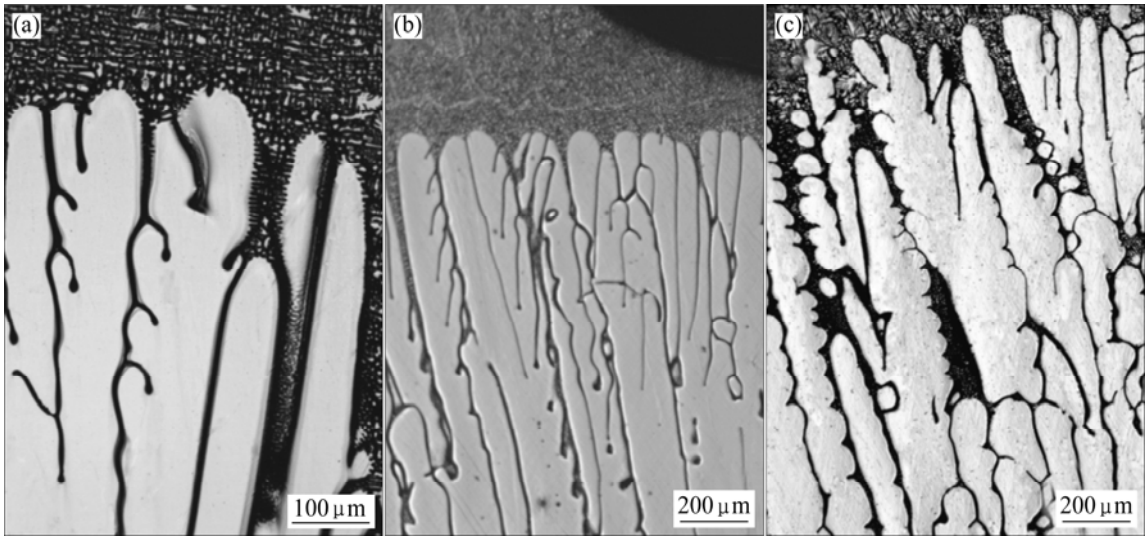

Fig.4 Effect of sample diameter on interface morphologies at v=15 μm/s: (a) d=1.8 mm; (b) d=3.5 mm; (c) d=7.2 mm

Table 1 Effect of sample diameter on PDAS under different withdrawal velocities

Sample diameter/mm	Primary dendrite arm spacing/μm				
	v=15 μm/s	v=30 μm/s	v=100 μm/s	v=300 μm/s	v=600 μm/s
1.8	61.7	75.6	91.9	62.8	44.1
3.5	78.1	113.5	118.8	88.9	61
7.2	95	130.3	140.2	102.9	75

increase in lower growth rate and then to decrease in higher growth rate. Therefore, the maximum of PDAS appears near the growth rate of 100 μm/s, as shown in Fig.5.

Besides, for constant growth rate, the primary dendrite is also refined with the decrease of the sample diameter. In other words, the smaller the sample diameter, the smaller the PDAS is. The relationship among PDAS, sample diameter and growth rate is shown in Fig.5.

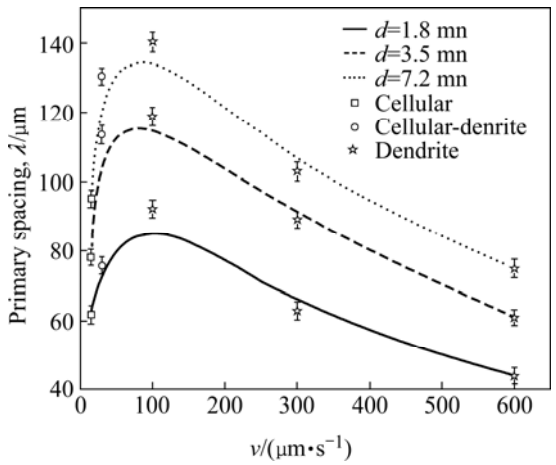

Fig.5 Variation of cellular/dendrite arm spacings with withdrawal velocity at different sample diameters

4 Discussion

4.1 Thermal gradient under different diameter of samples

According to the measured result of thermal gradient, the smaller the sample diameter, the higher the thermal gradient is at the given growth rate. Usually, thermal gradient is obtained from the heat balance at a planar liquid/solid interface, and the radial thermosolute convection is commonly neglected. Therefore, thermal gradient can be calculated by[19]

$$G_{\mathrm{L}}=\frac{1}{K_{\mathrm{L}}}\left(K_{\mathrm{S}}G_{\mathrm{S}}-\rho L_{\mathrm{f}}v\right)= \frac{1}{K_{\mathrm{L}}}\left[\frac{2h\alpha\left(T-T_0\right)}{v\cdot d}-\rho L_{\mathrm{f}}v\right] \quad (1)$$

where K_{S} and K_{L} are thermal conductivities of solid and liquid, respectively; h is coefficient of heat transfer; α is thermal coefficient of conduction, $\alpha=\dfrac{K_{\mathrm{S}}}{\rho_{\mathrm{s}}c_p}$; ρ is density; d is sample diameter; and L_{f} is latent heat.

As can be seen from Eq.(1), thermal gradient is dependent on heat transfer coefficient h, sample diameter d and growth rate v. Therefore, for the same processing technique and constant velocity, it can be controlled by sample diameter d only. Hence, thermal gradient is inverse to sample diameter for given alloy at constant velocity under certain processing technique, namely, the smaller sample diameter corresponds to higher thermal gradient.

Besides, in smaller samples, thermosolute convection is relatively weak[15−18]. But in larger sample, it can enable melt temperature to be much

uniform and greatly decrease the liquid temperature gradient. Hence, for the same material under the given condition, the smaller the sample diameter, the higher the thermal gradient is.

4.2 Relationship between primary dendrite arm spacing and sample diameter

With regard to calculating the primary dendrite spacing λ_1, scholars have tried to acquire a single value relationship. The first significant treatment to characterize primary spacing as a function of growth rate v, thermal gradient G and equilibrium solidification range of the alloy ΔT_0 was developed by HUNT[8]. Using the mass balance condition, and assuming that the region close to the tip can be approximated as part of sphere, HUNT[8] combined primary dendrite spacing with tip radius, and got primary dendrite spacing as follows:

$$\lambda_1 = 2.83\left(k\Delta T_0 D\Gamma\right)^{1/4} v^{-1/4} G^{-1/2} \tag{2}$$

where k is partition coefficient, D is diffusion coefficient in liquid, and Γ is Gibbs-Thomson coefficient.

Another detailed theoretical model to characterize the primary arm spacing was obtained by KURZ and FISHER[9], who assumed the shape of dendrite to be ellipsoids. Using the marginal stability criterion for an isolated dendrite, they obtained

$$\lambda_1 = 4.3\left(\Delta T_0 D\Gamma/k\right)^{1/4} v^{-1/4} G^{-1/2} \tag{3}$$

TRIVEDI[10] modified HUNT's model[8] using marginal stability criterion, and got

$$\lambda_1=2.38(\Delta T_0 kD\Gamma L)^{1/4} v^{-1/4} G^{-1/2} \tag{4}$$

where L=1/2(l+1)(l+2) for the spherical approximation of the dendrite front, l is the harmonic of perturbation. For dendrite, l=6.

AN and LIU[11] adopted HUNT's assumption[8] and TRIVEDI's tip composition[10], and obtained the result as

$$\lambda_1 = 1.34L^{1/2}\left(D\Gamma\Delta T_0\right)^{1/4} v^{-1/4} G^{-1/2} \tag{5}$$

In summary, all kinds of the above models can be summarized as $\lambda_1=k_x\Delta T_0^{1/4}/v^{-1/4}G^{-1/2}$, and the difference among them is the constant k_x only. That is partially because the sample diameter is ignored, but the tip shape is changed with sample diameter. For given alloy, the primary dendrite arm spacing is just correlated with growth rate v and thermal gradient G. What's more, it is inverse to thermal gradient. Therefore, for given alloy and growth rate, the smaller the sample diameter, the higher the thermal temperature is, and the finer the primary dendrite is. From the present experiment, the experimental results of λ_1 obtained in three diameters (1.8, 3.5 and 7.2 mm) of samples are compared with HUNT model, K-F model, TRIVEDI model and AN-LIU model, as shown in Fig.6 and Fig.7. It should be mentioned that, the aim of this work is to study the primary dendrite arm spacing, so cellular spacing is not analyzed in Fig.6 and

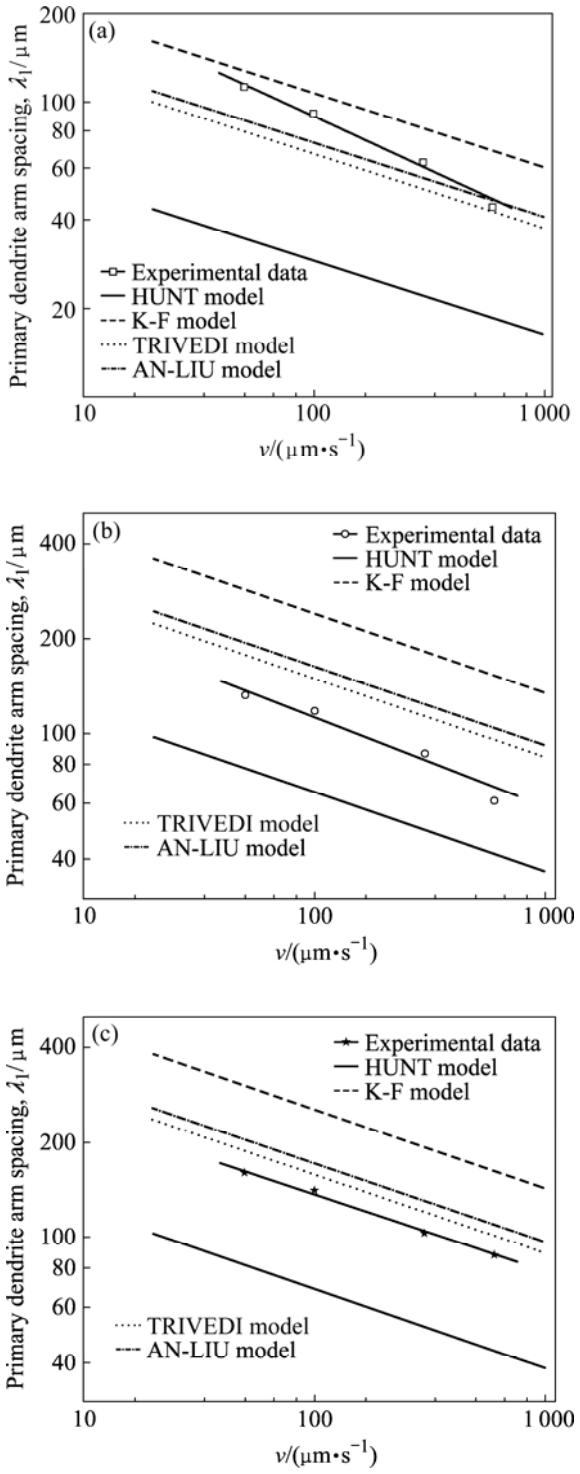

Fig.6 Comparison of experimental data and theoretical modes for primary dendrite spacings λ_1 varying with growth rates: (a) d=1.8 mm; (b) d=3.5 mm; (c) d=7.2 mm (Correlation parameters of data fitting (R^2) are 0.988 6, 0.953 6, and 0.993 7, respectively)

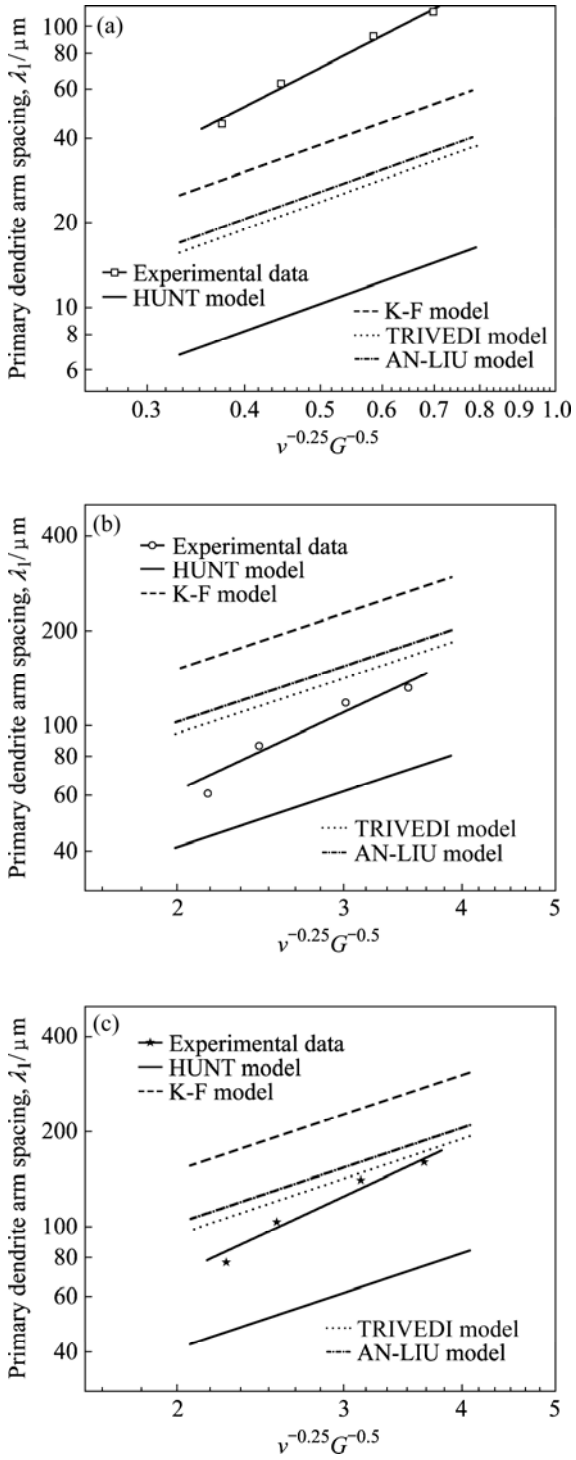

Fig.7 Comparison of experimental data and theoretical modes for primary dendrite spacings λ_1 varying with $v^{-0.25}G^{-0.5}$: (a) d=1.8 mm; (b) d=3.5 mm; (c) d=7.2 mm (Correlation parameter of data fitting (R^2) are 0.988 6, 0.935 3 and 0.954 8, respectively)

Fig.7. Fig.6 shows the variation of λ_1 with growth rate for different sample diameters, where λ_1 values are obtained both from experiments and theoretical models. As can be seen in Figs.6(a−c) (whose correlation parameters of data fitting (R^2) are 0.988 6, 0.953 6, and 0.993 7, respectively), with the increase of the growth rate, primary dendrite spacing tends to decrease.

From Fig.6, by making linear regression analysis, the relationship between PDAS and growth rate for samples with diameter of 1.8, 3.5 and 7.2 mm can be expressed in Eqns.(6−8), respectively:

$$\lambda_1=461.76v^{-0.35} \quad (6)$$

$$\lambda_1=417.92v^{-0.28} \quad (7)$$

$$\lambda_1=415.83v^{-0.25} \quad (8)$$

It is found that they all fit $\lambda_1=k_av^{-b}$, where k_a and b are constants for given alloy and thermal gradient. From Table 2, it can be seen that for Al-Cu alloys, b=0.28−0.38, but for other materials it is larger than 0.33. Moreover, k_{1-6} values in Table 2 are constants for given thermal gradient. But the present results are 0.25, 0.28 and 0.31, respectively. They are in quite good agreement with theoretical result b=0.25, especially for 7.2 mm diameter of sample. It is thus obtained that the present experimental values are valuable.

Table 2 Variation of primary dendrite arm spacing λ_1 with v for different materials

Composition	Primary dendrite spacing	Reference
Al-2%Cu	$\lambda_1=k_1v^{-0.28}$	[11]
Al-4.5%Cu	$\lambda_1=k_2v^{-0.38}$	[20]
Al-4.1%Cu	$\lambda_1=k_3v^{-0.40}$	[21]
Pb-40%Sn	$\lambda_1=k_4v^{-0.39}$	[22]
Pb-8%Au	$\lambda_1=k_5v^{-0.44}$	[23]
SCN-2.5%ETH	$\lambda_1=k_6v^{-0.33}$	[24]

Figs.7(a−c) show the variations of primary dendrite arm spacing with ($v^{-0.25}G^{-0.5}$) for sample diameter of 1.8 mm, 3.5 mm and 7.2 mm, respectively. It can be seen that an increase in ($v^{-0.25}G^{-0.5}$) produces primary dendrite arm spacing λ_1 increasing. To be mentioned, the thermal gradient G is varied with growth rate in this experiment.

In order to gain the relationship of experimental value λ_1 with G and v, we fit experimental results by linear regression shown in Fig.7, and the following equation are obtained:

For 1.8 mm diameter of sample,

$$\lambda_1=28.77v^{-0.35}G^{-0.70} \quad (9)$$

For 3.5 mm diameter of sample,

$$\lambda_1=23.17v^{-0.35}G^{-0.70} \quad (10)$$

For 7.2 mm diameter of sample,

$$\lambda_1=23.84v^{-0.35}G^{-0.70} \quad (11)$$

They all fit $\lambda_1=k_bv^{-a_1}G^{-b_1}$, where b_1/a_1=2, k_b, a_1 and b_1 are constants. Compared with Table 3, the relationship of previous primary dendrite spacing with v

Table 3 Variation of primary dendrite arm spacing λ_1 with temperature gradient G and velocity v for different alloys

Composition	Primary dendrite spacing	Reference
Al-2.4%Cu	$\lambda_1=k_7G^{-0.5}v^{-0.5}$	[25]
Al-4.4%Cu	$\lambda_1=k_8G^{-0.50}v^{-0.36}$	[25]
Al-10.1%Cu	$\lambda_1=k_9G^{-0.50}v^{-0.43}$	[25]
Al-4.5%Cu	$\lambda_1=k_{10}(Gv)^{-0.27}$	[26]
Al-11%Mg	$\lambda_1=k_{11}(Gv)^{-0.33}$	[27]
Al-(9.5−28.1)%Fe	$\lambda_1=k_{12}G^{-0.5}v^{-0.25}$	[4]
Ni base superalloy	$\lambda_1=k_{13}(Gv)^{-0.31}$	[28]

and G for Al-(9.5−28.1)%Fe fits $b_1/a_1=2$, which is the same as theoretical model. But for Al-4.4%Cu and Al-10.1%Cu, the values of b_1/a_1 are 1−2; however, they are all equal for Al-2.4%Cu, Al-4.5%Cu, Al-11%Mg and Ni base superalloy. It is worth to mention that k_{7-13} values in Table 3 are constants for given G. Actually, theoretical results show that $b_1/a_1=2$ results primary dendrite arm spacing, so there is some deviations in previous experimental values and theoretical results. In contrast to previous experimental values, the present results fit theoretical values well. It is even much worth to mention that the experimental results achieved by linear regression analysis method differ little from the theory: $a_1=0.35$, $b_1=0.70$. This indicates the conformability of experiment values is very well.

From Eqs.(6−11), it is acquired that the present values are valuable, thus the experimental values are compared with classical models to get the more suitable model for different sample diameters.

For sample with diameter of 1.8 mm, the experimental values are between K-F and AN-LIU model as shown in Fig.6(a). But for 3.5 mm and 7.2 mm sample, the experimental values of λ_1 are between HUNT and TRIVEDI model, and the values of λ_1 from K-F model are too large in comparison with experimental results (Figs.6(b) and (c)). The probable reason is that the hypothesized dendrite tip is ellipsoid rather than the paraboloid of revolution, and the sample diameter is not concerned, then the deviation occurs. TRIVEDI and AN-LIU model are very similar, because AN-LIU adopted TRIVEDI model's tip composition. Both of them are a little larger than experimental results, but TRIVEDI model are very close to the experimental value. However, HUNT model is obviously small compared with experimental results of all samples, as shown in Fig.6. Especially, for 3.5 mm sample, primary dendrite spacing λ_1 of sample with 7.2 mm in diameter is much close to TRIVEDI model. But for 1.8 mm sample diameter, there is a little difference from that of 3.5 mm and 7.2 mm samples, and the experimental results are relatively larger than those of other sample diameters. Compared with all the models, they are close to K-F model.

In Fig.7, for sample with diameter of 3.5 mm and 7.2 mm, the experimental values are between HUNT and TRIVEDI model, but much closer to TRIVEDI model as shown in Figs.7(b) and (c), whose correlation parameter of data fitting (R^2) are 0.935 3 and 0.954 8, respectively. Compared with experimental values of 7.2 mm sample, the variational trend of experimental values of 3.5 mm sample is much similar to that of theoretical results. However, for 1.8 mm sample diameter, as shown in Fig.7(a), whose correlation parameter of data fitting (R^2) is 0.988 6, experimental values are closer to K-F model. Because the sample diameter is too small to measure the thermal gradient, it could be only roughly estimated from Eq.(1), so there probably exists some difference from real thermal gradient. Thus, for both 3.5 mm and 7.2 mm sample diameters, the values are close to TRIVEDI model. However, for 1.8 mm sample diameter, experimental values are larger than those of all of the models, but much closer to K-F model.

Hence, a conclusion can be drawn that the sample diameter is significantly affect primary dendrite arm spacing, and it should not be ignored for calculating PDAS. For all the classical models, K-F model fits for very thin sample ($d<2$ mm), where convection is weak, but for larger sample diameters ($d>2$ mm) where convection should be considered, it seems that TRIVEDI model describes PDAS better.

5 Conclusions

1) At the same growth rate, primary dendrite arm spacing is decreased with the decrease of the sample diameter.

2) The relationships of primary dendrite spacing with growth rate and thermal gradient obtained for three sample diameters (1.8 mm, 3.5 mm and 7.2 mm) are $\lambda_1=28.77v^{-0.35}G^{-0.70}$, $\lambda_1=23.17v^{-0.35}G^{-0.70}$, and $\lambda_1=23.84v^{-0.35}G^{-0.70}$, respectively. They all fit $\lambda_1=k_bv^{-a_1}G^{-b_1}$, where $b_1/a_1=2$, k_b, a_1 and b_1 are constants

3) K-F model fits for PDAS in small sample size ($d<2$ mm) under which convection is weak, whereas for larger sample size ($d>2$ mm) where convection should be considered, TRIVEDI model describes PDAS better.

Acknowledgements

The authors are grateful to Dr. LUO W Z, Dr. ZOU M M and Dr. CUI J for their experimental assistance.

References

[1] BUCHMANN M, RETTENMAYR M. Microstructure evolution during melting and resolidification in a temperature gradient [J]. J Cryst Growth, 2005, 284: 544−553.

[2] SPINELLI J E, PERES M D, GARCIA A. Thermosolutal convective effects on dendritic array spacings in downward transient directional solidification of Al-Si alloys [J]. J Alloy Comp, 2005, 403: 228−238.

[3] GÜNDÜZ M, ÇADIRLI E. Directional solidification of aluminum-copper alloys [J]. Mater Sci Eng, 2002, 327A: 167−185.

[4] LIANG D, JIE W Q, JONES H. The effect of growth velocity on primary spacing of Al_3Fe dendrites in hypereutectic Al-Fe alloys [J]. J Cryst Growth, 1994, 135: 561−564.

[5] ÜSTÜN E, ÇADIRLI E, KAYA H. Dendritic solidification and characterization of asuccinonitrile-acetone alloy [J]. J Phys: Condens Matter, 2006, 18: 7825−7839.

[6] SUN M J, PARK Y M, KIM Y D. Dendrite spacing and microstructure evolution dependent on specimen history [J]. Script Mater, 2007, 57: 985−987.

[7] DING G L, HUANG W D, LIN X, ZHOU Y H. Prediction of average spacing for constrained cellular/dendritic growth [J]. J Cryst Growth, 1997, 177: 281−288.

[8] HUNT J D. Solidification and casting of metals [M]. London: The Metals Society, 1979: 3−9.

[9] KURZ W, FISHER D J. Dendrite growth at the limit of stability: Tip radius and spacing [J]. Acta Metall, 1981, 29: 11−20.

[10] TRIVEDI R. Interdendritic spacing: Part II. A comparison of theory and experiment [J]. Metall Trans, 1984, 15A: 977−982.

[11] AN G Y, LIU L X. Dendrite spacing in unidirectionally solidified Al-Cu alloy [J]. J Cryst Growth, 1987, 80: 383−392.

[12] WARREN J A, LANGER J S. Stability of dendritic arrays [J]. Phys Review, 1990, 42A: 3518−3525.

[13] WARREN J A, LANGER J S. Prediction of dendritic spacing in a directional solidification experiment [J]. Phys Review, 1993, 47E: 2702−2712.

[14] HUNT J D, LU S Z. Numerical modeling of cellular/dendritic array growth: Spacing and structure predictions [J]. Metall Mater Trans, 1996, 27A: 611−623.

[15] CHEN J, SUNG P K, TEWARI S N, POIRIER D R, DE GROHIII H C. Directional solidification and convection in small diameter crucibles [J]. Mater Sci Eng, 2003, 357A: 397−405.

[16] NGUYEN T H, DABO Y, DREVET B, DUPOUY M D, CAMEL D, BILLIA B, HUNT J D, CHILTON A. Directional solidification of Al-1.5wt%Ni alloys under diffusion transport in space and fluid-flow localization on earth [J]. J Cryst Growth, 2005, 281: 654−668.

[17] LIU S, MAZUMDER P, TRIVEDI R. A new thermal assembly design for the directional solidification of transparent alloys [J]. J Cryst Growth, 2002, 240: 560−568.

[18] TRIVEDI R, MAZUMDER P, TEWARI S N. The effect of convection on disorder in primary cellular and dendritic arrays [J]. Metall Mater Trans, 2002, 33A: 3763−3775.

[19] ZHANG W G, LIU L, HUANG T W, ZHANG J H. Determining the temperature measurement of temperature gradient on the ZMLMC directional solidification apparatus and the effect of temperature gradient on solidification microstructure [J]. Foundry Technology, 2006, 27: 1165−1168.

[20] LIN X, HUANG W, FENG J, LI T, ZHOU Y. History-dependent selection of primary cellular/dendritic spacing during unidirectional solidification in aluminum alloys [J]. Acta Mater, 1999, 47: 3271−3280.

[21] MIYATA Y, SUZUKI T, UNO J I. Cellular and dendritic growth: Part I. Experiment [J]. Metall Trans. 1985, 16A: 1799-1805.

[22] MASONJ T, VERHOEVEN J D, TRIVEDI R. Primary dendrite spacing I. Experimental studies [J]. J Cryst Growth, 1982, 59: 516−524.

[23] KLAREN C M, VERHOEVEN J D, TRIVEDI R. Primary dendrite spacing of lead dendrites in Pb-Sn and Pb-Au alloys [J]. Metall Trans, 1980, 11A: 1853−1861.

[24] HUANG W D, GENG X G, ZHOU Y H. Primary spacing selection of constrained dendritic growth [J]. J Cryst Growth, 1993, 134: 105−115.

[25] YOUNG K P, KIRKWOOD D H. The dendrite arm spacing of aluminum-copper alloys solidified under steady-state conditions [J]. Metall Trans, 1975, 6A: 197−205.

[26] SU R J, OVERFELT R A, JEMIAN W A. Microstructure and compositional transients during accelerated directional solidification of Al-4.5wt% Cu [J]. Metall Trans, 1998, 29A: 2375−2381.

[27] LIU Y L, KANG S B. Solidification and segregation of Al-Mg alloys and influence of alloy composition and cooling rate [J]. Mater Sci Tech, 1997, 13: 331−336.

[28] KERMANPUR A, VARAHRAAM N, ENGILEHEI E, MOHAMMADZADEH M, DAVAMI P. Directional solidification of Ni base superalloy IN738LC to improve creep properties [J]. Mater Sci Tech, 2000, 16: 579−586.

(Edited by YANG Bing)